ELSEVIER

European Journal of Radiology 70 (2009) 101–110

EJR
EUROPEAN JOURNAL OF RADIOLOGY

www.elsevier.com/locate/ejrad

Texture analysis in non-contrast enhanced CT: Impact of malignancy on texture in apparently disease-free areas of the liver

Balaji Ganeshan [a,*], Kenneth A. Miles [b,1], Rupert C.D. Young [a,2], Chris R. Chatwin [a,3]

[a] *Department of Engineering & Design, University of Sussex, Falmer, Brighton BN1 9QT, UK*
[b] *Division of Clinical & Laboratory Sciences, Brighton & Sussex Medical School, University of Sussex, Falmer, Brighton BN1 9PX, UK*

Received 31 May 2007; received in revised form 10 December 2007; accepted 11 December 2007

Abstract

Objectives: To determine whether texture analysis of non-contrast enhanced computed tomography (CT) images in apparently disease-free areas of the liver is altered by the presence of extra- and intra-hepatic malignancy in colorectal cancer patients.
Materials and methods: Hepatic attenuation and texture were assessed from non-contrast enhanced CT in three groups of colorectal cancer patients: (A) 15 controls with no malignancy; (B) nine patients with extra-hepatic malignancy but no liver involvement; (C) eight patients with hepatic metastases. Regions of interest were manually constructed only over apparently normal areas of liver tissue excluding major blood vessels and areas of intra-hepatic fat, which may otherwise alter CT texture irrespective of the presence of malignancy. Texture was analysed on unfiltered images and following band-pass image filtration to highlight image features at different spatial frequencies (fine: 2 pixels/1.68 mm in width, medium: 6 pixels/5.04 mm and coarse: 12 pixels/10.08 mm). The relative contributions made to the image by features at two different spatial frequencies were expressed as filter ratios (fine/medium, fine/coarse and medium/coarse). Texture was quantified as mean grey-level intensity, entropy and uniformity.
Results: Texture was not altered on unfiltered images whereas relative texture analysis following image filtration identified differences in fine to medium texture ratios in apparently disease-free areas of the liver in patients with hepatic metastases as compared to patients with no tumour (entropy, $p = 0.0257$) and patients with extra-hepatic disease (uniformity, $p = 0.0143$).
Conclusions: Relative texture analysis of unenhanced hepatic CT can reveal changes in apparently disease-free areas of the liver that have previously required more complex perfusion measurements for detection.
© 2007 Elsevier Ireland Ltd. All rights reserved.

Keywords: Colorectal cancer; Computed tomography (CT); Image processing; Computed-assisted; Texture analysis

1. Introduction

In western countries, colorectal cancer is the second most common malignancy [1]. Up to 40% of the patients undergoing resection of the primary tumour will relapse and die of their disease, making colorectal cancer the second leading cause of death related to cancer [2]. The liver is the sole site of secondary tumour spread (i.e. metastasis) in 20–40% of patients [3] and therefore it is a common practice to follow-up patients after their curative resection. There is an overall survival benefit for intensifying the follow-up of such patients with imaging of the liver being associated with reduced mortality (odds ratio = 0.66, 95% confidence limits 0.46–0.95) [4]. The American Society of Clinical Oncology (ASCO) advises annual computed tomography (CT) of the chest and abdomen for 3 years for patients having a higher risk of recurrence after primary therapy [5]. Therefore during re-staging of patients with colorectal cancer, CT of the liver is widely employed as a means of diagnosing hepatic metastases.

Alterations in hepatic contrast enhancement and perfusion in morphologically normal livers have been shown to herald the subsequent development of overt metastases and identify colorectal patients with reduced survival [6–8]. Such techniques could be included within the conventional CT examination recommended by ASCO and so potentially improve the effectiveness of surveillance. However, wider adoption of these

* Corresponding author. Tel.: +44 1273 872642; fax: +44 1273 690814.
E-mail addresses: b.ganeshan@sussex.ac.uk (B. Ganeshan), k.a.miles@bsms.ac.uk (K.A. Miles), r.c.d.young@sussex.ac.uk (R.C.D. Young), c.r.chatwin@sussex.ac.uk (C.R. Chatwin).
[1] Tel.: +44 1273 877574; fax: +44 1273 877576.
[2] Tel.: +44 1273 678908; fax: +44 1273 690814.
[3] Tel.: +44 1273 678901; fax: +44 1273 690814.

0720-048X/$ – see front matter © 2007 Elsevier Ireland Ltd. All rights reserved.
doi:10.1016/j.ejrad.2007.12.005

techniques has been constrained by the additional complexity and cost along with the increased radiation burden to the patient, as compared to the standard contrast enhanced protocols used in clinical practice. Furthermore, in some patients use of contrast agents required for these techniques is contraindicated either due to allergy or other complications such as renal failure. Therefore a method that provides comparable information without the need for administration of contrast media would be desirable.

Visual analysis of diagnostic images is largely based upon evaluating morphological information such as size and shape. Image perception and identifying relationships between perceived patterns and possible diagnosis heavily depend on radiologist's knowledge, analytical skills, memory, intuition and diligence. However, the human visual system has difficulties in discriminating textural information such as coarseness and regularity that result from local spatial variations in image brightness [9]. Furthermore, quantitative information from images is becoming increasingly important. This however is not possible through visual analysis and therefore requires computer-based algorithmic processing. In medical image processing, texture analysis (TA) is a vital component of computer-assisted diagnosis (CAD) because it is difficult to classify human tissues based on shape or grey-level information given in Hounsfield units (HU) only. Also, improvements in texture analysis techniques would increase the extracted information enabling better quantification of differences in appearance inaccessible to the naked eye.

Most CAD–TA algorithms follow a two stage scheme with initial quantification using numerous mathematical descriptors of texture computed from different available texture analysis methods and subsequent decision algorithms based on computer vision and artificial intelligence. The three general methods of texture quantification follow model based, frequency based, structure based or statistically based approach [10,11]. In model based approach, mathematical models such as fractal and stochastic models, analyze texture by identifying an appropriate model that reflects prior information about the type of tissue images to be analyzed [12–15]. These are computationally complex, lack feature selectivity and are not suitable for describing local image structures. Furthermore frequency domain power spectrum analysis or structural methods are less employed because medical image data is not periodic with individual pixel values reflecting image intensity and the variations in medical images account for functional or pathological characteristics which lack any definite shape, whereas a statistical approach measuring spectral properties of an image has been commonly employed in texture quantification [16–18]. But the effectiveness of these texture analysis methods and texture parameters in discriminating various pathological states of the tissue depends on the application under study and their ability to be readily applicable to diagnostic images in routine clinical practice. Several methods of texture analysis such as Wavelet techniques and decision-based algorithms have previously been applied to the liver on CT, mostly for identification and characterization of focal liver lesions [19–25]. Few studies have focused on texture changes in apparently disease-free areas of the liver [26–28]. Some studies have combined multiple texture parameters, for example using classifiers and artificial neural networks (ANNs) [19–21,24,25]. However, acceptance of such methods in the clinical arena is constrained by the lack of any clear biological correlate for the successful combination of texture features. On the other hand, a previous computer simulation of hepatic CT has shown that simple statistical texture parameters correlate with liver vascularity [29]. This finding was subsequently confirmed in humans by a report showing correlations between CT hepatic texture and blood flow [30]. Thus these methods benefit from a direct correspondence to the blood flow changes previously observed in disease-free areas of the liver on CT in patients with hepatic metastases [31–33] and therefore have been adopted for this study. Because there are no recognized biological correlates for any alternative approaches to texture analysis in liver CT, we have not included a comparator texture analysis methodology for this study.

Of the previous studies demonstrating alterations in CT texture in apparently disease-free areas of the liver, one did not state whether contrast material had been given whilst others reported significant differences on contrast enhanced images, thus preventing its application when contrast enhancement may not be indicated, for example during integrated positron emission tomography (PET)–CT, or when enhancement has been contraindicated. Furthermore, neither study assessed the potential impact of extra-hepatic disease on liver texture.

We have recently developed and implemented a method for texture analysis of medical images that employs selective-scale filtration similar to the Wavelet approach to separately extract fine to coarse features in the image and uses statistical texture parameters to quantify textures at different texture scales. This selective-scale incremental tuning ability of the filter (which is not a feature of orthogonal Wavelet basis), benefits from independent assessment of fine, medium and coarse textures corresponding to particular scales of detail whilst minimizing the effects of noise. This study assesses the potential for this approach to texture analysis of non-contrast enhanced CT images to reveal differences between normal liver and apparently disease-free areas of the liver in patients with either hepatic or extra-hepatic metastases from colorectal cancer.

2. Materials and methods

The study comprised texture analysis of archival image data that had been acquired as part of a research program in which patients underwent a diagnostic CT examination of the chest, abdomen and pelvis that included images of the liver before and during intravenous contrast enhancement, along with a Fluoro-deoxy-glucose (FDG)–PET examination of the whole body. This research program had been approved by the Hospital Ethics Committee with informed written consent obtained from all patients. The study consisted of 40 patients under imaging surveillance following previous resection of colorectal cancer. Based on the visual interpretation of the diagnostic CT and FDG–PET, these patients were divided in the following groups: group A: patients with no current evidence of tumour ($n = 15$); group B: patients with metastases at sites remote from the liver but without liver metastases ($n = 9$) and group C: patients with

liver metastases with or without extra-hepatic metastases ($n = 8$). Eight patients were excluded either due to the presence of a focal lesion in the CT slice under consideration or due to motion artefacts.

2.1. CT image acquisition

The non-contrast enhanced images were used for texture analysis and comprised a 10 mm section of mid liver obtained with a 1 s scan duration, at a tube current of 300 mA and tube voltage of 120 kVp (CT Twin: Elscint, Haifa, Israel). Only a single non-contrast enhanced image through the mid-liver was obtained in order to minimise the additional radiation burden beyond the standard clinical protocol which, at this institution, comprised contrast enhanced images only. The in-plane pixel resolution for the liver images used in this study was 0.84 mm. Reconstructed images were transferred to a personal computer for texture analysis.

2.2. Texture analysis

Texture was assessed in apparently disease-free areas of the liver tissue from non-contrast enhanced CT images. Texture analysis within hepatic region of interest (ROI) comprised processing the CT image to produce a series of derived images displaying fine, medium and coarse texture features respectively (Fig. 1). This methodology was implemented with a dedicated program written using MATLAB (Math works Inc, Natick, USA), a high-level technical computing language and interactive development environment to perform image processing. This texture analysis methodology employed in this study is described in detail below. However, in brief the texture in each derived image was quantified by calculating the mean grey-level intensity (i.e. brightness), entropy (i.e. intensity and inhomogeneity) and uniformity (i.e. distribution of grey-level) within the ROI. Entropy and uniformity represent additional statistical image parameters that can quantify homogeneity and brightness; features that are perceived visually as image texture which give further insight into the distribution of tissue attenuation that is lost when averaging intensity over a large area. Whilst little used in clinical radiology to date, the term "entropy" has been widely applied in information theory as a useful measure of the scatter of the elements in an image [34]. Texture ratios were also calculated from individual derived images, i.e. fine to medium, fine to coarse and medium to coarse. These values can be considered to represent the relative contribution made by fine, medium and coarse texture components, respectively.

Texture analysis comprised two stages: (a) image filtration, followed by (b) quantification of texture. A thresholding procedure was carried out to exclude fat, air and bone and include liver blood vessels by removing from analysis any pixels with attenuation values below 0 HU or above 300 HU in the unfiltered image. Even after applying this threshold statistically large number of liver pixels was available for reliable texture analysis. Quantification of texture was performed with and without image filtration

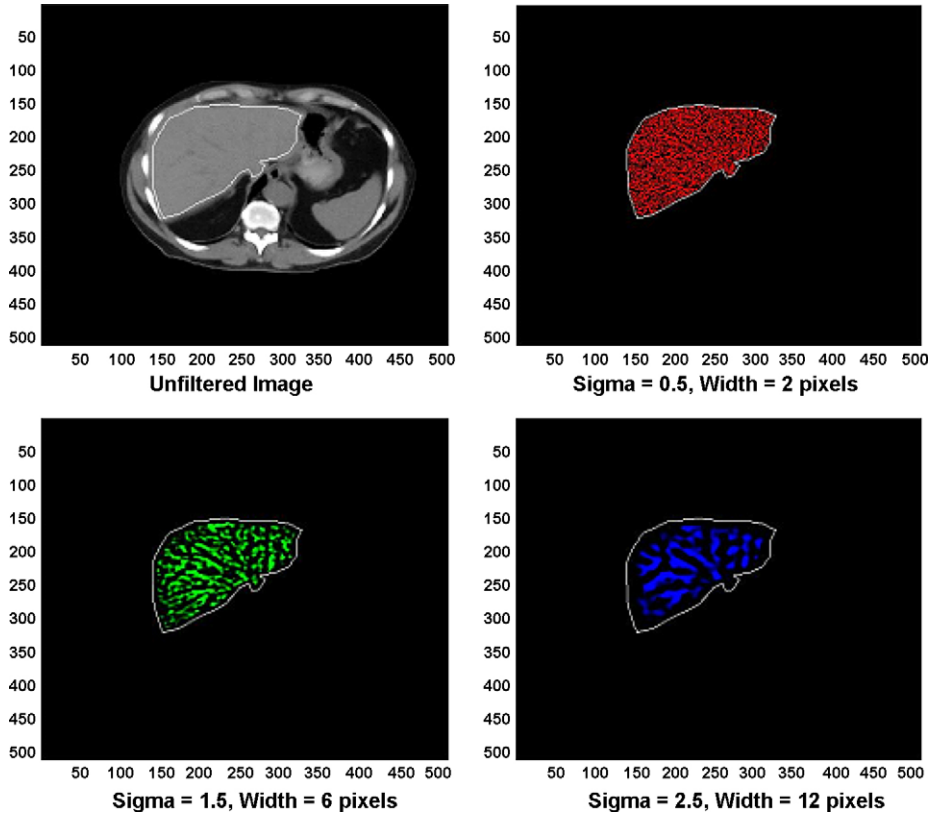

Fig. 1. Unfiltered and filtered images at different sigma values in the non-contrast enhanced image.

2.2.1. Image filtration

There are different transform methods available for texture analysis such as Fourier [35] and Wavelet transforms [36–39] to obtain derived textured images. Frequency domain methods perform poorly in practice, due to lack of spatial localisation. Wavelet transforms provide better spatial localisation and have advantages of varying the spatial resolution to represent textures at the most suitable scale and wide range of choices for the Wavelet function. However, Wavelets are generally orthogonal filters restricted in the freedom of selectively tuning the filter. This drawback can be avoided by choosing a Laplacian of Gaussian [40] spatial filter as a non-orthogonal Wavelet filter.

2.2.2. Laplacian of Gaussian (LoG) band-pass filter [40]

We have used Laplacian of Gaussian band-pass filter for our texture analysis. This is a combination of Laplacian, which is a differential operator used for detecting intensity changes within an image first smoothened by the Gaussian distribution, based on the filter sigma value. The degree or strength of smoothening is proportional to the filter sigma value. For example, small sigma value produces a lower degree of smoothening enabling extraction of fine texture, while higher sigma value produces greater degree of smoothening enabling extraction of coarse texture. This filter is explained in detail below.

The two-dimensional (2D) Gaussian distribution (G) is given by

$$G(x, y) = e^{-(x^2+y^2)/2\pi\sigma^2} \quad (1)$$

where (x, y) are the spatial coordinates of the image array and sigma (σ) is the standard deviation. The 2D Gaussian distribution effectively blurs the image, wiping out all structures at scales much smaller than the sigma of the Gaussian. Thus the Gaussian distribution would enable highlighting only hepatic textural features of a particular scale in CT images corresponding to the σ value. To assess independently whether different scales of liver texture from apparently disease-free areas of non-contrast enhanced CT images could differentiate between the diagnostic groups of patients, we have employed this LoG filtration technique to filter out textural features at different scales. Gaussian smoothening, which has the desirable characteristics of being smooth and localized in both the spatial and frequency domains was employed before the Laplacian operator.

Laplacian (∇^2) was chosen as it is the lowest-order orientation-independent (isotropic) differential operator which inherently has less computational burdens and can be used to detect intensity changes in an image that correspond to the zero-crossings of the filter [40]. $\nabla^2 G$ is the Laplacian of Gaussian

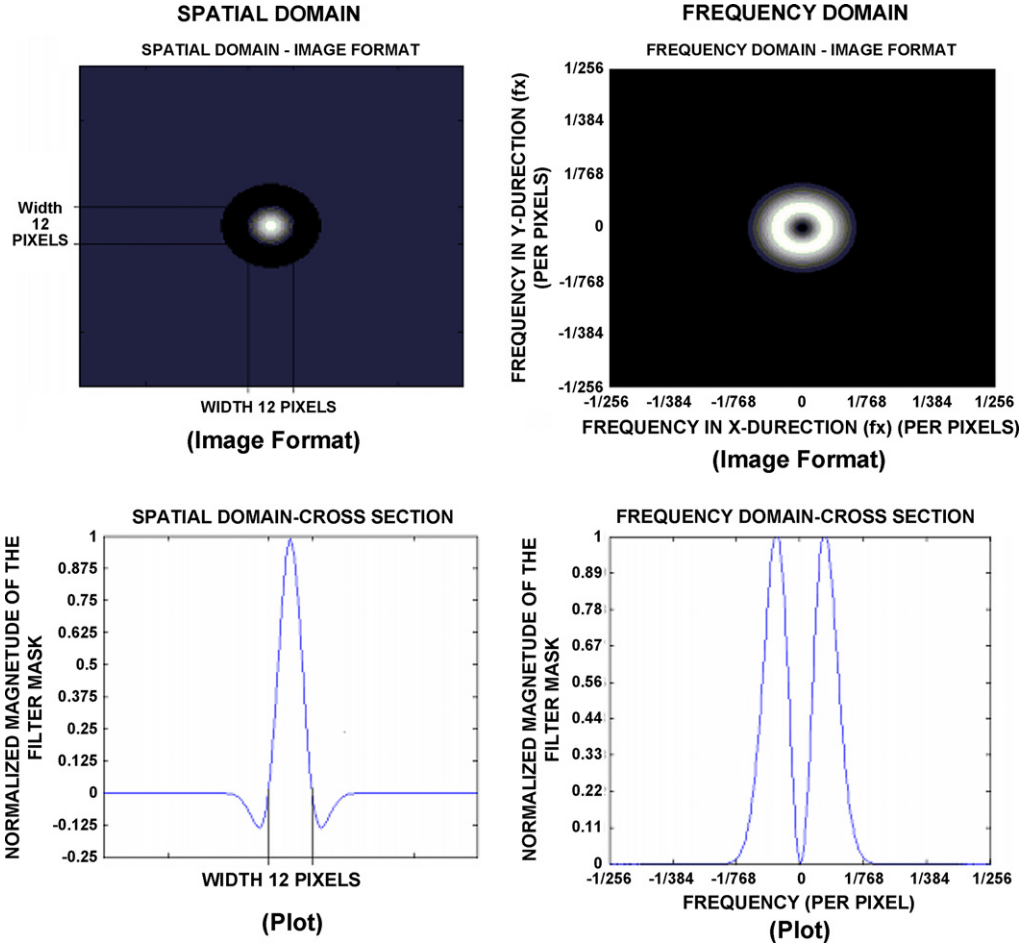

Fig. 2. The 2D forms of the LoG filter in the spatial and frequency domain at sigma (σ) value of 2.5.

Table 1
Filter sigma value and the corresponding width of the filter (in pixels and mm)

Sigma (σ)	Texture type	Filter width (pixels)	Filter width (mm)
0.5	Fine	2	1.68
1.5	Medium	6	5.04
2.5	Coarse	12	10.08

(LoG) filter, a circularly symmetric Mexican-hat-shaped filter (see Fig. 2 for spatial and frequency domain representations of the filter) whose distribution in 2D spatial domain is given by

$$\nabla^2 G(x, y) = \frac{-1}{\pi\sigma^4}\left(1 - \frac{x^2 + y^2}{2\sigma^2}\right) e^{-(x^2+y^2)/2\sigma^2} \quad (2)$$

From the mathematical expression of this circularly symmetric filter at three different sigma (σ) values, the number of pixels representing the width between the diametrically opposite zero-crossing points in this filter can be calculated in the spatial domain (see Fig. 2). The width of the filter at different σ values are obtained by evaluating the LoG spatial distribution along the x and y directions. The lower the sigma value, the smaller is the width of the filter in the spatial domain and the larger is the pass-band region of the filter in the frequency domain, highlighting fine details or features of the filtered image in the spatial domain. Similarly, the higher the sigma value, the higher is the width of the filter in the spatial domain; this corresponds to a smaller pass-band region of the filter in the frequency domain, highlighting coarse features of the filtered image in the spatial domain. Thus the filter can be modulated so as to highlight fine ($\sigma = 0.5$), medium ($\sigma = 1.5$) and coarse ($\sigma = 2.5$) liver textures or features. Table 1 indicates the filter width in pixels for the sigma values 0.5, 1.5 and 2.5. From Fig. 2 it is shown that the width of the filter at a particular sigma value is the distance between the diametrically opposite zero-crossings, which are obtained by evaluating the LoG spatial distribution along the x and y directions. This width can be considered as the scale at which the structures in the image will be highlighted and enhanced whilst structures below this scale will become blurred (see Fig. 1).

Filtration can be done in the spatial or frequency domain. In the spatial domain, the filter mask is convolved with the image, which involves intensive computation. It is more efficient to employ the filter in the frequency domain, as convolution of the filter mask and the image in the spatial domain is equivalent to multiplication of the Fourier transforms of the filter mask and the image in the frequency domain. The inverse Fourier transform of the filtered spectrum gives the resultant filtered image in the spatial domain. Also the accuracy of this filtration operation is improved when implemented in the frequency domain, as the quantization errors arising from the convolution in the spatial domain for the small σ values being considered will result in inaccuracies of the filtered image.

2.2.3. Quantification of texture

For each patient from the three diagnostic groups, a hepatic ROI excluding the inferior vena cava, porta hepatis, visible metastases and areas of fat (e.g. adjacent to the falciform ligament) was manually drawn on the non-contrast enhanced image of each patient within the margins of the liver and stored in the computer as a binary mask and assigned to the corresponding patient. The presence of fat and major blood vessels may alter apparently disease-free areas of the liver texture on CT. This ensured that the same unmodified ROI corresponding to each patient was used for all the different two-dimensional (2D) texture analyses which were carried out on the same non-contrast enhanced image from which the binary mask was generated. The resulting images, containing only liver pixels, underwent band-pass filtering with the LoG filter using sigma values of 0.5 (fine texture), 1.5 (medium texture) and 2.5 (coarse texture). The following statistical parameters were used to evaluate texture within the hepatic region of interest, both for unfiltered images as well as filtered images highlighting fine, medium and coarse texture, respectively: (a) mean grey-level intensity (m), (b) Entropy (e), a parameter indicating intensity and inhomogeneity (irregularity), and (c) Uniformity (u) indicating how close the image is to a uniform distribution of the grey-levels. These parameters are defined below where R the region of interest within the image $a(x, y)$, N the total number of pixels in the region of interest R, l the number of grey-levels (for example $l = 1$ to k indicates grey-level from 1 to k) in the region of interest R and $p(l)$ the probability of the occurrence of the grey-level l based on the image histogram technique:

$$\text{Mean grey-level intensity } (m) = \frac{1}{N}\sum_{(x,y)\in R}[a(x, y)] \quad (3)$$

$$\text{Entropy } (e) = -\sum_{l=1}^{k}[p(l)]\log_2[p(l)] \quad (4)$$

$$\text{Uniformity } (u) = \sum_{l=1}^{k}[p(l)]^2 \quad (5)$$

In addition to the quantification of fine, medium and coarse texture highlighted at different band-pass regions of the filter; the ratios of texture parameters highlighted by different band-pass regions of the filter, i.e. fine to medium, fine to coarse and medium to coarse were quantified which are defined as follows:

$$\text{Fine to medium texture ratio for mean grey-level intensity} = \frac{1/N\sum_{(x,y)\in R}[a(x, y)_{\sigma=0.5}]}{1/N\sum_{(x,y)\in R}[a(x, y)_{\sigma=1.5}]} \quad (6)$$

$$\text{Fine to medium texture ratio for entropy} = \frac{-\sum_{l=1}^{k}[p(l)_{\sigma=0.5}]\log_2[p(l)_{\sigma=0.5}]}{-\sum_{l=1}^{k}[p(l)_{\sigma=1.5}]\log_2[p(l)_{\sigma=1.5}]} \quad (7)$$

$$\text{Fine to medium texture ratio for uniformity} = \frac{\sum_{l=1}^{k}[p(l)_{\sigma=0.5}]^2}{\sum_{l=1}^{k}[p(l)_{\sigma=1.5}]^2} \quad (8)$$

Fine to coarse texture ratio for mean grey-level intensity

$$= \frac{1/N\sum_{(x,y)\in R}[a(x,y)_{\sigma=0.5}]}{1/N\sum_{(x,y)\in R}[a(x,y)_{\sigma=2.5}]} \quad (9)$$

Fine to coarse texture ratio for entropy

$$= \frac{-\sum_{l=1}^{k}[p(l)_{\sigma=0.5}]\log_2[p(l)_{\sigma=0.5}]}{-\sum_{l=1}^{k}[p(l)_{\sigma=2.5}]\log_2[p(l)_{\sigma=2.5}]} \quad (10)$$

Fine to coarse texture ratio for uniformity

$$= \frac{\sum_{l=1}^{k}[p(l)_{\sigma=0.5}]^2}{\sum_{l=1}^{k}[p(l)_{\sigma=2.5}]^2} \quad (11)$$

Medium to coarse texture ratio for mean grey-level intensity $= \frac{1/N\sum_{(x,y)\in R}[a(x,y)_{\sigma=1.5}]}{1/N\sum_{(x,y)\in R}[a(x,y)_{\sigma=2.5}]}$ (12)

Medium to coarse texture ratio for entropy

$$= \frac{-\sum_{l=1}^{k}[p(l)_{\sigma=1.5}]\log_2[p(l)_{\sigma=1.5}]}{-\sum_{l=1}^{k}[p(l)_{\sigma=2.5}]\log_2[p(l)_{\sigma=2.5}]} \quad (13)$$

Medium to coarse texture ratio for uniformity

$$= \frac{\sum_{l=1}^{k}[p(l)_{\sigma=1.5}]^2}{\sum_{l=1}^{k}[p(l)_{\sigma=2.5}]^2} \quad (14)$$

These texture ratio quantifications were used because the ratios would be effectively normalized, thereby minimizing the effects of any potential variations in CT attenuation values occurring from one patient to another and also reducing the effect of noise on texture quantification. Also texture parameters from unfiltered images provided a control state against which the benefits gained from image filtration were assessed.

2.3. Statistical analysis

For all three diagnostic groups of patients, medians ± interquartile range were calculated for each texture parameter for the unfiltered, filtered—fine, medium and coarse texture images along with ratios of texture parameters from fine and medium, fine and coarse and medium and coarse images. The non-parametric two-tailed Mann Whitney test was used for evaluating the significance of the difference between the groups on the basis of their texture without filtration, filtered texture and texture ratios besides gender, age and body weight. The difference between groups was considered to be significant if the p-value was less than 0.05. For texture parameters demonstrating significant differences between the diagnostic groups, the receiver-operating characteristics (ROC) analysis identified diagnostic thresholds to identify patients with hepatic metastases. These predictors were also evaluated using a 2×2 contingency table from which sensitivity and specificity values were calculated and their significance tested using Fisher's exact two-tailed test. Also, for these diagnostic thresholds the odds ratio and 95% confidence interval were calculated.

3. Results

Out of the eight patients excluded from the initial dataset of 40, six were from group C each having a focal liver lesion within the CT slice selected for texture analysis, and of the remaining two with severe motion artefacts on the CT image, one was from group A and other from B. There was no difference in gender, age or body weight between the three groups based on Mann Whitney test (Table 2).

The texture parameters for unfiltered and filtered non-contrast enhanced CT images for all the three diagnostic groups are summarized in Table 3. There were no significant differences for the texture parameters between any groups for texture analysis of unfiltered images and there was no difference between groups A (no tumour) and B (extra-hepatic tumour only) for any texture parameter.

For coarse and medium texture images, there was a trend towards higher values for mean grey-level intensity and entropy in group C (liver metastases) as compared to groups A and B, reaching statistical significance for coarse texture ($p < 0.05$). On the other hand, in fine texture images, these parameters tended to be lower in group C. Uniformity values also tended to be lower in group C for coarse and medium texture images but not reaching statistical significance.

Greater separation of the patient groups was achieved by using ratios of texture values. In particular, fine to medium texture ratios were most significant in differentiating the different diagnostic groups (see Table 3 and Figs. 3–5). For comparison between groups A and C, the most significant difference was obtained for the ratio of fine to medium texture using the texture parameter entropy ($p = 0.0257$) whilst the difference in this ratio for mean grey-level intensity was less significant ($p = 0.049$). For groups B and C, the most significant difference was obtained using the fine to medium texture ratio for the texture parameter

Table 2
Patient characteristics

	Group A: normal patients	Group B: patients with extra-hepatic metastases	Group C: patients with liver metastases
Number	15	9	8
Sex, male	7	7	4
Median age (range)	60 (46–70)	63 (54–73)	64 (46–81)
Median weight (range)	79 (56–109)	77 (59–95)	77 (47–99)

No significant difference was observed between the three diagnostic groups for gender, age and body weight based on Mann Whitney test.

Table 3
Texture parameters mean grey-level intensity, entropy and uniformity measured for texture analysis with and without image filtration

Texture	Parameter	Group A Median	Group B Median	Group C Median
Without filtration	Mean grey-level intensity	25.4363	27.1292	33.0651
	Entropy	4.8046	4.8838	4.68295
	Uniformity	0.042788	0.041746	0.045969
Fine ($\sigma = 0.5$)	Mean grey-level intensity	6.0004	5.5249	5.46295
	Entropy	3.2648	3.2131	3.1756
	Uniformity	0.31033	0.31343	0.30914
Medium ($\sigma = 1.5$)	Mean grey-level intensity	2.8296	2.6531	3.1023
	Entropy	2.5853	2.521	2.64225
	Uniformity	0.40014	0.40043	0.37238
Coarse ($\sigma = 2.5$)	Mean grey-level intensity	1.9789	1.8777	2.7034 a*
	Entropy	2.0138	2.032	2.2377 a*
	Uniformity	0.51072	0.48171	0.472375
Fine/medium	Mean grey-level intensity	2.197785	2.049123	1.698856 a*
	Entropy	1.298338	1.280643	1.183054 a**, b**
	Uniformity	0.769779	0.781044	0.811117 b***
Fine/coarse	Mean grey-level intensity	3.148519	2.969172	1.89672 a*, b*
	Entropy	1.611122	1.563338	1.383165 a*, b*
	Uniformity	0.613353	0.607295	0.657135
Medium/coarse	Mean grey-level intensity	1.532863	1.448996	1.20652 a*, b**
	Entropy	1.244492	1.211374	1.173022
	Uniformity	0.788798	0.815011	0.800232

a and b: statistically significant difference in value from group A and group B patients, respectively (*, $0.03 < p < 0.05$; **, $0.02 < p < = 0.03$; ***, $p = 0.01$).

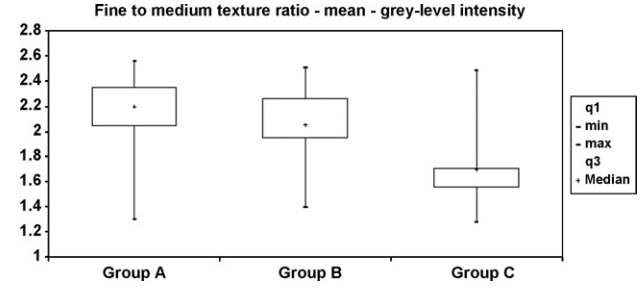

Fig. 3. Mean grey-level intensity for fine to medium texture ratio ($\sigma = 0.5$ and 1.5) in the non-contrast enhanced images for the three groups of patients. The patients with liver metastases (group C) showed a significantly decreased trend in ratio values compared with the normal patients (group A; $p = 0.0488$). Box and whisker chart showing median, inter-quartile range and range.

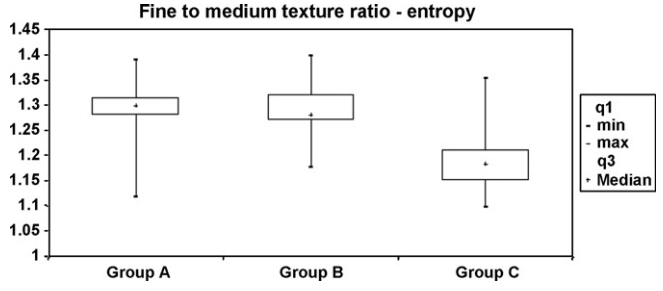

Fig. 4. Entropy for fine to medium texture ratio ($\sigma = 0.5$ and 1.5) in the non-contrast enhanced images for the three groups of patients. The patients with liver metastases (group C) showed a significantly decreased trend in ratio values compared with the normal patients (group A; $p = 0.0257$) and with the patients with extra-hepatic metastases (group B; $p = 0.03$). Box and whisker chart showing median, inter-quartile range and range.

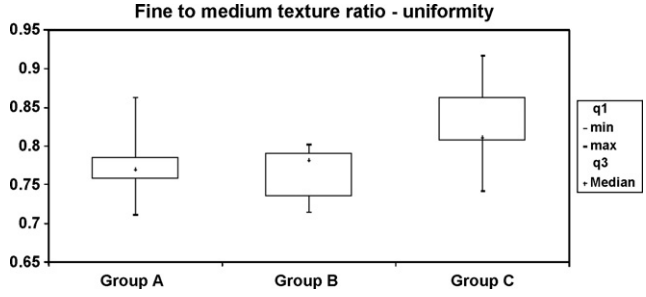

Fig. 5. Uniformity for fine to medium texture ratio ($\sigma = 0.5$ and 1.5) in the non-contrast enhanced images for the three groups of patients. The patients with liver metastases (group C) showed a significantly increased trend in ratio values compared with the patients with extra-hepatic metastases (group B; $p = 0.0143$). Box and whisker chart showing median, inter-quartile range and range.

uniformity ($p = 0.0143$). Entropy also discriminated these two groups, with the highest significance obtained using the fine to medium texture ratio ($p = 0.03$).

For fine to medium texture ratios, an entropy value of less than 1.21 identified patients with liver metastases (group C) from the rest of the patients (area under ROC curve = 0.802, $p < 0.0005$, sensitivity = 75%, specificity = 83%, odds ratio = 15, 95% confidence interval = 2.18–103 with $p < 0.005$). The diagnostic performance of the three texture parameters is summarized in Table 4.

4. Discussion

The analysis methodology used in this study has demonstrated statistically significant differences in the texture of

Table 4
Diagnostic performances of texture parameters obtained from fine to medium texture ratios in identifying patients with liver metastases

Texture parameter	AUC (p)	Diagnostic threshold	Sensitivity	Specificity	Odds ratio	95% confidence interval	Fisher's test (p)
Mean Grey-level Intensity	0.760 (<0.005)	<1.71	75% (6/8)	83.33% (20/24)	15	2.18–103	<0.005
Entropy	0.802 (<0.0005)	<1.21	75% (6/8)	83.33% (20/24)	15	2.18–103	<0.005
Uniformity	0.781 (<0.01)	>0.80	75% (6/8)	87.50% (21/24)	21	2.82–156	<0.0025

AUC: Area under the receiver-operating characteristics (ROC) curve.

apparently disease-free areas of the liver tissue in patients with metastases as compared to patients with no evidence of tumour and patients with extra-hepatic tumour only in the absence of contrast enhancement. These texture findings are directly analogous to the perfusion CT findings of Tsushima et al. [33]. However, by avoiding the multi-phase acquisitions using contrast media that are needed to assess hepatic haemodynamics on CT, texture analysis from a single non-contrast enhanced image is associated with a lower radiation burden and cost. The fact that changes in texture are detectible in CT images acquired without contrast enhancement means that information comparable to that derived from perfusion imaging can be obtained in patients for whom administration of contrast agents is contra-indicated. One reason for the alteration in non-contrast enhanced CT texture of apparently disease-free areas of the liver tissue could be due to the presence of abnormalities in the hepatic parenchyma not easily perceived by the eye. The possibility that liver texture is altered by humoral factors secreted by tumours is unlikely because such factors would be expected to alter texture in apparently disease-free areas of the liver for all patients with evidence of tumour, irrespective of its location within or outside the liver. We found no change in texture in association with extra-hepatic tumour, a finding that is in accordance with Tsushima et al. [33] who found no blood flow changes in a similar patient group.

The alterations in texture parameters seen in apparently disease-free areas of the liver in patients with liver metastases are found not only on fine texture images (approximately 2 mm) but also on the medium and coarse texture images which highlight image features of approximately 5–10 mm. However, the changes in fine texture parameters tend to be in an opposite direction to the alterations in medium and coarse texture. For example, mean grey-level intensity is reduced on fine texture images in apparently normal liver in patients with metastases (Group C) but increased in medium and coarse texture images. On unfiltered images, these opposite effects would tend to cancel out but would be compounded when fine to medium and fine to coarse texture ratios are calculated.

The texture analysis methodology used in our study is simple, easy to implement and effective but differs from the previous studies demonstrating alterations in texture in apparently normal liver in patients with metastases [26,27]. Firstly, we have used image filtration to separately evaluate fine, medium and coarse texture. This filtration proved to be critical in our study as no significant differences were found between any of the diagnostic groups for texture analysis of unfiltered images. Also, the previous study of Mir et al. [26] found that second order direction-oriented statistical parameters (i.e. statistical methods based on the joint probability distributions of pairs of pixels such as grey-level run length or co-occurrence matrices) were necessary to extract relevant textural features from liver regions. By using image filtration in our texture analysis, we were able to use first order statistical parameters based on the probability distributions of individual pixels such as mean grey-level intensity, entropy and uniformity. These parameters have the advantage of being directionally independent and less computationally expensive. There is no a priori reason to indicate that changes in liver parenchyma in association with hepatic metastases should be associated with any particular direction and indeed are more likely to be non-directional. Therefore, our employment of a directionally independent filter and first order statistical parameters can be considered appropriate. Furthermore, the use of ratios of texture parameters, derived from images filtered to highlight different degrees of spatial detail (i.e. fine to medium, fine to coarse and medium to coarse ratios) to analyze texture in non-contrast hepatic CT, were more effective in differentiating the diagnostic groups than parameters derived from individual filtered images. Among the different texture ratios, fine to medium texture ratios tended to highlight textural differences between the two liver areas better than fine to coarse and medium to coarse texture ratios.

Our study was constrained by a small sample size. However the series was a part of a research protocol where all the patients underwent CT and PET imaging irrespective of their CT findings, on the basis of which patients were divided into three diagnostic groups. It is unlikely that the results obtained were due to a chance alone as statistically significant differences between the diagnostic groups were observed for several texture parameters with fine to medium texture ratios providing the best discrimination. Nevertheless our findings need to be confirmed in a larger series of similar patients. A further limitation of our study has been the inability to confirm the actual causes in alteration in texture in the apparently disease-free areas of the liver in patients with overt lesions. Biopsy of these regions was prevented by ethical considerations. However, it may be possible to address this issue in future by studying CT texture in apparently normal liver regions in patients undergoing resection of hepatic metastases in whom pathological examination of equivalent liver regions could be undertaken. We were also unable to determine whether changes in hepatic texture heralded the subsequent development of over lesions as this follow-up information was not available with the archival images used in this study.

In the United States, it is estimated that 148,610 new cases of colorectal cancer are identified each year [1]. The majority of these patients will undergo hepatic CT at some stage in their clinical care. Because of a greater sensitivity for hep-

atic metastases, such CT examinations are ideally performed following intravenous administration of contrast media. However, the use of contrast media is contraindicated in patients with allergy, renal failure or other disorders. Contraindications to iodinated contrast media for patients undergoing CT occur with sufficient frequency for gadolinium to be proposed as an alternative agent for CT angiography [41,42]. For example, Remy-Jardin et al. [41] identified 39 such patients referred for CT pulmonary angiography within one year. However, gadolinium is not currently considered a suitable alternative to iodinated contrast media for opacification of parenchymal organs such as the liver [42]. Thus, texture analysis of CT images without contrast media could be usefully applied to patients with contraindications to iodinated contrast media referred for hepatic CT.

The use of non-contrast enhanced images for texture analysis avoids any potential variability in the results arising from individual patient physiological characteristics that are known to affect contrast enhancement. The significant differences in texture parameters for patients without liver metastases from apparently normal liver in patients with liver metastases found in our study suggest that texture analysis of conventional CT examinations without contrast-agents could be potentially employed as a computer-assisted diagnosis (CAD) technique for preliminary examination of colorectal cancer patients. CT images acquired without contrast material are less likely to detect liver metastases than those obtained with contrast enhancement. A finding of altered texture on non-contrast enhanced CT images in patients unable to receive contrast agents due to allergy, renal failure or other contra-indication, or performed as part of PET–CT, would indicate an increased risk of undetected hepatic metastases. For example, based on our data, an entropy value below 1.21 would indicate a 15-fold increase in risk of undetected hepatic metastases, identifying metastases elsewhere in the liver with a sensitivity of 75% and specificity 83%. This increased risk may warrant further investigation with another imaging modality such as magnetic resonance imaging (MRI), which has greater sensitivity for small hepatic metastases, and for which the likelihood of adverse reaction is less. Should subsequent MRI demonstrate focal liver lesions, these patients could potentially be candidates for liver biopsy or radiofrequency ablation.

5. Conclusions

In summary, this study has shown the ability of texture analysis of non-contrast enhanced CT images of the liver to reveal changes in apparently disease-free areas of the liver in colorectal cancer patients with liver metastases as compared to those with no evidence of tumour or extra-hepatic tumour only. Although the findings are comparable to those previously described using CT perfusion imaging, texture analysis can be readily applied to images acquired in routine practice, thereby reducing cost, complexity and radiation burden. Abnormal texture in the absence of visible metastases on non-contrast enhanced CT could potentially be used as an indication for further investigation with hepatic MRI.

Acknowledgements

The research was funded by NHS Research & Development and by Brighton & Sussex Medical School.

References

[1] Jemal A, Murray T, Ward E, et al. Cancer statistics, 2005. CA Cancer J Clin 2005;55:10–30.
[2] Obrand D, Gordon P. Incidence and patterns of recurrence following curative resection of colon cancer. Dis Colon Rectum 1997;40:15–24.
[3] Morgan-Parkes JH. Metastases: mechanisms, pathways, and cascades. Am J Roentgenol 1995;164(5):1075–82.
[4] Jeffrey GM, Hickey BE, Hider P. Follow-up strategies for patients treated for non-metastatic colorectal cancer (Cochrane review). In: The Cochrane library. Oxford: Update Software; 2003 [issue 2].
[5] Desch CE, Benson III AB, Somerfield MR, et al. American society of clinical oncology. Colorectal cancer surveillance: 2005 update of an American society of clinical oncology practice guideline. J Clin Oncol 2005;23:8512–9.
[6] Platt JF, Francis IR, Ellis JH, Reige KA. Liver metastases: early detection based on abnormal contrast material enhancement at dual-phase helical CT. Radiology 1997;205:49–53.
[7] Sheafor DH, Killius JS, Paulson EK, DeLong DM, Foti AM, Nelson RC. Hepatic parenchymal enhancement during triple-phase helical CT: can it be used to predict which patients with breast cancer will develop hepatic metastases? Radiology 2000;214:875–80.
[8] Miles KA, Colyvas K, Griffiths MR, Bunce IH. Colon cancer: risk stratification using hepatic perfusion CT. Eur Radiol 2004;14(Suppl. 2):129.
[9] Tourassi GD. Journey towards computer-aided diagnosis: role of image texture analysis. Radiology 1999;213:317–20.
[10] Van Gool L, Dewaele P, Oosterlink A. Texture analysis Anno 1983. Comput Vis Graph Image Process 1985;29:337–57.
[11] Reed TR, Hans Du Bui JM. A review of recent texture segmentation and feature extraction techniques. Comput Vis Graph Image Process 1993;57:359–72.
[12] Cross G, Jain A. Markov random field texture models. IEEE Trans Pattern Anal Mach Intell 1983;5(1):25–39.
[13] Pentland A. Fractal-based description of natural scenes. IEEE Trans Pattern Anal Mach Intell 1984;6(6):661–74.
[14] Chellappa R, Chatterjee S. Classification of textures using Gaussian Markov random fields. IEEE Trans Acoust Speech Signal Process 1985; 33(4):959–63.
[15] Derin H, Elliot H. Modeling and segmentation of noisy and textured images using Gibbs random fields. IEEE Trans Pattern Anal Mach Intell 1987;9(1):39–55.
[16] Coleman AJ, Tonge KA, Rankin SC. The power spectral density as a measure in computed tomographic scans of liver. Br J Radiol 1982;55:601–3.
[17] Weszaka JS, Dyer CR, Rosenfeld A. A comparative study of texture measures for terrain classification. IEEE Trans Syst Man Cyber SMC 1976;6(4):269–85.
[18] Conners RW, Harlow CA. A theoretical comparison of texture algorithms. IEEE Trans Pattern Anal Mach Intell PAMI 1980;2(3):204–22.
[19] Bilello M, Gokturk SB, Desser T, Napel S, Jeffrey Jr RB, Beaulieu CF. Automatic detection and classification of hypodense hepatic lesions on contrast-enhanced venous-phase CT. Med Phys 2004;31(9):2584–93.
[20] Gletsos M, Mougiakakou SG, Metsopoulos GK, Nikita KS, Nikita AS, Kelekis D. A computer-aided diagnostic system to characterise CT focal liver lesions: design and optimisation of a neural network classifier. IEEE Trans Inf Technol Biomed 2003;7(3):153–62.
[21] Klein HM, Klose KC, Eisele T, Brenner M, Ameling W, Gunther RW. The diagnosis of focal liver lesions by the texture analysis of dynamic computed tomograms. Rofo 1993;159(1):10–5 [Article in German].
[22] Kim T, Federle MP, Baron RL, Peterson MS, Kawamori Y. Discrimination of small hepatic hemangiomas from hypervascular malignant tumours smaller than 3 cm with three-phase helical CT. Radiology 2001;219:699–706.

[23] Semler L, Dettori L, Furst J. Wavelet-based texture classification of tissues in computed tomography. IEEE CBMS 2005:265–70.
[24] Afaq Hussain S, Shigeru E. Use of neural networks for feature based recognition of liver region on CT images. Neural Networks for Signal Processing X, 2000. In: Proceedings of the 2000 IEEE Signal Processing Society Workshop, vol. 2. 2000. p. 831–40.
[25] Mala K, Sadasivam V. Automatic segmentation and classification of diffused liver diseases using wavelet based texture analysis and neural network. In: Proceeding of the INDICON, 2005 Annual IEEE. 2005. p. 216–9.
[26] Mir AH, Hanmandlu M, Tandon SN. Texture analysis of CT-images for early detection of liver malignancy. Biomed Sci Instrum 1995;31:213–7.
[27] Ganeshan B, Miles KA, Young RCD, Chatwin CR. Hepatic entropy and uniformity: additional parameters that can potentially increase the utility of contrast enhancement during abdominal CT. Clin Radiol 2007;62(8):761–8.
[28] Ganeshan B, Miles KA, Young RCD, Chatwin CR. In search of biologic correlates for liver texture on portal-phase CT. Acad Radiol 2007;14(9):1058–68.
[29] Bezy-Wendling J, Kretowski M, Rolland Y, Le Bidon W. Towards a better understanding of texture in vascular CT scan simulated images. IEEE Trans Biomed Eng 2001;48:120–4.
[30] Ganeshan B, Miles KA, Young RCD, Chatwin CR. Hepatic enhancement in colorectal cancer: texture analysis correlates with hepatic hemodynamics and patient survival. Acad Radiol 2007;14(12):1520–30.
[31] Platt JF, Francis IR, Ellis JH, Reige KA. Difference in global hepatic enhancement assessed by dynamic CT in normal subjects and patients with hepatic metastases. J Comput Assist Tomogr 1997;21(3):348–54.
[32] Leggett DAC, Kelley BB, Bunce IH, Miles KA. Colorectal cancer: diagnostic potential of CT measurements of hepatic perfusion and implications for contrast enhancement protocols. Radiology 1997;205:716–20.
[33] Tsushima Y, Blomley MJK, Yokoyama H, Kusano S, Endo K. Does the presence of distant and local malignancy alter parenchymal perfusion in apparently disease-free areas of the liver? Dig Dis Sci 2001;46(10):2113–9.
[34] Shannon CE. Communication in the presence of noise. Proc Inst Radio Eng 1949;37:10–21.
[35] Rosenfeld A, Weszka J. Picture recognition. In: Fu K, editor. Digital pattern recognition. Springer-Verlag; 1980. p. 135–66.
[36] Mallat S. Multi-frequency channel decomposition of images and wavelet models. IEEE Trans Acous Speech Signal Process 1989;37(12):2091–110.
[37] Laine A, Fan J. Texture classification by wavelet packet signatures. IEEE Trans Pattern Anal Mach Intell 1993;15(11):1186–91.
[38] Lu C, Chung P, Chen C. Unsupervised texture segmentation via Wavelet transform. Pattern Recogn 1997;30(5):729–42.
[39] Strang G, Nguyen T. Wavelets and filter banks. Wellesley-Cambridge Press; 1996.
[40] Marr D. Representing the image: zero-crossings and the raw primal sketch. In: Wilson J, Monsour P, editors. Vision. San Francisco: W.H. Freeman and Company; 1982. p. 54–68.
[41] Remy-Jardin M, Dequiedt P, Ertzbischoff O, et al. Safety and effectiveness of Gadolinium-enhanced multi-detector row spiral CT angiography of the chest: Preliminary results in 37 patients with Contr-indications to iodinated contrast agents. Radiology 2005;235:819–26.
[42] Rosioreanu A, Alberico RA, Litwin A, Hon M, Grossman ZD, Katz DS. Gadolinium-enhanced computed tomographic angiography: current status. Curr Probl Diagn Radiol 2005;34:207–19.